Modelling the Performance of a Continuously Variable Supercharger Drive System

ATJM Rose, S Akehurst, CJ Brace

University of Bath

Abstract

This paper details a simulation based investigation into a novel forced induction boosting system with a centrifugal-type supercharger driven from the engine crankshaft via a continuously variable transmission (CVT). This system acts as a pre-boost to a traditional fixed geometry turbocharger and has been identified as a possible solution to improving low speed engine torque and transient response of future downsized and existing turbocharged engines. The concept was modelled around an existing baseline high speed direct injection (HSDI) diesel engine model featuring a variable geometry turbocharger (VGT).

Conclusions are drawn comparing the potential of the proposed system to the baseline engine in terms of brake specific fuel consumption (BSFC), and both steady state and transient performance. A design of experiments approach is applied to investigate the effect of supercharger compressor size, turbocharger compressor and turbine size, CVT ratio and engine compression ratio on the system performance. Optimisation techniques are then applied to identify the best settings for these parameters in the proposed system. Transient simulation was undertaken in a Matlab/Simulink Ricardo WAVE co-simulation environment to develop the required control strategies for the CVT supercharger.

The proposed system demonstrates a significant improvement in low speed engine torque and transient response of the boosting system during tip-in pedal events, which it is proposed will result in significant improvement in vehicle performance and driveability.

Keywords
Internal combustion engine; diesel engines; downsizing; supercharging; turbocharging; continuously variable transmission; simulation.

1 Introduction

Governments throughout the world are implementing legislation for ever more strict limits for vehicle emissions [1, 2], and it is only a matter of time before financial penalties are introduced to help motivate manufacturers to reduce the levels of carbon dioxide produced by their vehicles [3]. These factors combined with the need to remain profitable in the current global economic climate present automotive manufacturers with a significant challenge.

Engine downsizing is the process by which the speed and load operating point is shifted to a more efficient region through a reduction in engine displacement [4]. Full load performance is usually maintained through exhaust gas turbocharging to high boost pressures. Many authors, including Wijetunge et al. [5] have noted that 'engine downsizing has been identified as a viable, cost-effective method for the automotive industry to meet the increasingly stringent emissions and fuel economy targets stipulated by legislation throughout the world'.

Turbocharging can improve efficiency as well as power density by harnessing exhaust gas energy that would otherwise be wasted. There is, however, a fundamental compromise involved with matching a turbocharger to an engine: between power at high engine speeds and torque at low speed [5]. A large turbocharger offers the power at high speed, but suffers from poor low speed performance and transient response due to the lack of exhaust gas flow to overcome the inertia of the system. On the other hand a small turbocharger provides improved low speed torque and transient response due to the reduced inertia, but at high engine speeds would require turbine bypassing to prevent excessive turbocharger speed, thus sacrificing efficiency. With highly boosted engines this low speed performance impairment is compounded [6]. Ideally for a forced induction engine, the driveability

characteristics of a comparable naturally aspirated unit are an aim and a number of solutions have been introduced to diminish the effects of this turbocharging compromise.

As the name suggests, the variable geometry turbocharger (VGT) has a mechanism by which the effective turbine area (or aspect ratio) can be changed to produce the behaviour of a small or large turbocharger. Thus performance can be greatly improved over the entire speed range compared with an equivalent fixed geometry unit. However, this system still relies on the build-up of exhaust gas energy [7] and consequently does not completely solve the problem of low speed transient response.

There are many arrangements involving multiple turbochargers [8]; for the problem being considered at this juncture, a sequential system is the most appropriate for review. In a sequential arrangement a combination of two different sized turbochargers is used, switching between them based on engine speed. The smaller unit provides the torque at low engine speed and correspondingly good transient response due to its low rotational inertia; the larger unit utilises the higher exhaust gas flow at higher engine powers. However, as with a VGT the transient response of these systems is still ultimately limited by the available exhaust gas energy [5].

Mechanical supercharging offers increased power density similar to exhaust gas turbocharging, but without the detrimental effects on transient response. However, since the compressor is driven from the engine crankshaft, power is drawn from the useful output of the engine instead of utilising ‘free’ exhaust gas energy. Positive displacement units offer a relatively constant level of boost since they pump air at a fixed rate relative to engine speed and supercharger size. The main disadvantage (other than the parasitic losses incurred) is their size and weight relative to the boost provided. Centrifugal superchargers are generally more efficient, smaller and lighter than their positive displacement counterparts; the drawback being that boost increases with the square of the rotational speed, resulting in low boost at low engine speed. However, it has been suggested that a centrifugal supercharger

be driven through a variable transmission to allow the boost to be optimised throughout the entire engine speed range [9].

Combined charging systems involving a switchable mechanical supercharger used in conjunction with a conventional turbocharger have been well researched, particularly for heavy duty diesel applications [6, 7, 10]. Substantial improvements have been found in both steady state and transient performance at low engine speed [10], as well as engine braking performance [6]. Volkswagen has successfully implemented this technology on its 1.4 litre gasoline TSI 'Twincharged' engine, claiming it delivers the equivalent performance of a naturally aspirated 2.3 litre engine, but with a significant drop in fuel consumption [11]. Typically for this type of combined system a positive displacement-type supercharger is used. It seems that arrangements involving a centrifugal supercharger have not yet been researched – and certainly not with drive transmitted through a continuously variable transmission (CVT). It is this concept – as shown in the schematic diagram in Figure 1 – that has been investigated.

It is worth noting that designs involving an electrically driven compressor in place of the mechanical supercharger have also been investigated, yielding similar performance benefits [5]. It is proposed that a mechanical arrangement has significant advantages over electrical supercharger drives, operating with higher speed turbo-machinery solutions. The CVT driven supercharger is considered beneficial over electrical driven alternatives due to its ability to be operated continuously without issues of electrical heating, battery depletion or upgrading of the standard vehicle electrical architecture.

2 Steady State Simulation

2.1 System Model

The analysis was based on a previously validated [12] Ricardo WAVE engine model of a 2.0 litre in line 4 cylinder high speed direct injection (HSDI) diesel engine, employing common rail fuel injection and a variable geometry turbocharger – see Table 1. The combustion

process was described using a correlational compression ignition Wiebe model, whereby ignition delay and premixed burn fraction are computed using the fuel cetane number and in-cylinder temperature and pressure [13].

The standard engine model was run at a range of engine speeds along the limited torque curve (LTC) to provide a baseline for the performance characteristics. The twincharged concept was modelled by modifying the baseline model. The standard intercooler was duplicated and placed between the two compressors to account for the increase in charge temperature caused by the additional compressor. To avoid the complexities of adapting the control of the variable geometry rack position to the new configuration, the turbine was made pseudo-fixed geometry by setting the mechanism to fully open.

A bypass valve arrangement was implemented around the supercharger, the purpose of which is to allow the supercharger to be disengaged once it has reached the limits of its speed and mass flow range, and the intake air flow to be uninterrupted. By this stage – around 3000 rpm at full load – the turbocharger provides sufficient boost unaided. A magnetic clutch, similar to those used on automotive air-conditioning compressors, would allow the supercharger to be engaged and disengaged depending upon engine speed and load requirements. This type of arrangement has been previously explored by various groups [6, 7, 10], and is also in place on the Volkswagen TSI engine mentioned above [11].

As this investigation was to assess the potential of the concept, the original turbo-machinery was retained (with the supercharger compressor a duplication of the original turbocharger compressor); the WAVE software allows turbo-machinery components to be ‘scaled’, producing the effect of having a different size of compressor or turbine, but with similar flow characteristics. Scaling has the following effects:

For mass flow:
$$\dot{m}_{corr} = \dot{m}_{act} \sqrt{\frac{T_{in,act}}{T_{in,ref}}} \frac{P_{in,ref}}{P_{in,act}} \left(\frac{d_{ref}}{d_{act}} \right)^2 \quad (1)$$

For speed: $$n_{corr} = n_{act} \frac{d_{act}}{d_{ref}} \sqrt{\frac{T_{in,ref}}{T_{in,act}}} \quad (2)$$

For torque: $$\tau_{corr} = \tau_{act} \left(\frac{d_{ref}}{d_{act}} \right)^3 \frac{P_{in,ref}}{P_{in,act}} \quad (3)$$

In which $\frac{d_{act}}{d_{ref}}$ is defined as the scale factor (SF).

For inertia: $$I_{turb\_act} \propto m_{turb\_ref} \left(\frac{d_{turb\_act}}{d_{turb\_ref}} \right)^5 \quad (4)$$

$$I_{comp\_act} \propto m_{comp\_ref} \left(\frac{d_{comp\_act}}{d_{comp\_ref}} \right)^5 \quad (5)$$

It is assumed that isentropic efficiency is unaffected by the scaling process.

2.2 Design of Experiment Turbo-machinery Optimisation

The next stage was to apply design of experiments (DoE) techniques to optimise the scaling factors of the turbo-machinery, as well as reducing the geometric compression ratio of the engine to account for the increased boost pressures. The complex interdependence of each of the parameters to be optimised necessitated a formal approach. The ranges for the eight input parameters are specified in Table 2.

The Matlab Model Based Calibration (MBC) toolbox was used to develop the experimental test plan and to fit a response model to the acquired data. An initial simulation screening experiment of 250 points of a grid-type ‘optimal’ design was used to fill the corners and outer edges of the design space; these were then augmented with 750 points determined using a Halton Sequence ‘space-filling’ design to maximise coverage of the variables’ ranges in the most efficient way.

The responses of significant engine variables (such as brake torque and peak cylinder pressure) were subsequently modelled. For the majority of the variables a neural network

modelling approach was required due to the high complexity of the system – a result of the number of input parameters.

Once the response models had been evaluated satisfactorily they were imported into the calibration generation (CAGE) element of MBC, to form the plant model for the subsequent optimisation process. A sum optimisation method was applied to maximise the sum total of the modelled torque response over the engine speed range. The engine speed variable was changed in increments of 250 rpm in the range 1000-4500 rpm. Using a sum optimisation (as opposed to a point-to-point optimisation where torque would be maximised for each operating point individually) allowed the constraints of constant turbo-machinery scaling factors and compression ratio to be applied across the speed range. Otherwise these variables would be allowed to fluctuate with each operating point.

2.2.1 Performance Constraints

The following constraints were imposed upon the analysis in order to provide realistic and reasonable results:

- Maximum cylinder pressure < 160 bar
- Air-fuel ratio (AFR) > 17:1

160 bar peak cylinder pressure was deemed an acceptable limit given that much higher pressures (180-200 bar) have been demonstrated on both standard production and research engines [14, 15]. The 17:1 AFR limit was imposed as a smoke limitation measure, and was based on the lowest value of the baseline engine. Together with these absolute limits, at each stage the CVT ratios were evaluated to ensure they were within a feasible range. Furthermore, a torque limit of 400 Nm was applied to avoid excessive transmission loads.

Table 3 shows the parameters obtained from the optimisation process. The supercharger has been reduced in size by some 10%, relative to the original compressor, while the turbocharger compressor has increased by 7.5% and the turbine reduced by 7%. A slightly

reduced compression ratio of 18:1 was found to maintain the engine within the maximum cylinder pressure constraint. The supercharger size was reduced in order to provide the required pressure ratios at low mass flow (i.e. low engine speed) within surge limits. The turbocharger compressor has increased in size to take advantage of the potential to increase mass flow at high engine speeds without having to accommodate for the pressure ratios normally required at low speed.

2.3 Simulation Results

Running the twincharged WAVE model with the optimised parameters produces a torque curve significantly enhanced over the baseline – up until 3000 rpm, the point of supercharger disengagement (Figure 2a). Peak torque has been increased by 15% and is produced at a lower engine speed – down from 2000 rpm to 1500 rpm. More crucially, 90% of the peak value is available at 1000 rpm, compared with 50% for the baseline engine. However, the twincharged system is virtually identical to the original model past the point of supercharger disengagement. This is predominantly due to the rudimentary way in which the original turbocharger was adapted for this purpose – using a turbine and housing combination designed for a VGT as a fixed geometry unit is less than ideal. This is primarily manifested in the isentropic efficiencies of the turbine: the maximum efficiency is 65%, occurring when the variable geometry mechanism is around 30-70% open; maximum efficiency is just 55% when fully open. (A similar problem is encountered in a computational study by Millo et al. [16], albeit when modelling an electrical turbocompounding system.) At full load, the VGT of the baseline engine operates in the region of greatest efficiency (as shown in Figure 2b), whereas the twincharged engine is always operating in the off-design, fully open condition. As a result of these shortcomings, the modified turbocharger was unable to produce the same mass flow (and pressure ratio) as the original VGT, as Figure 2c shows. However, maintaining the fuelling rate of the baseline engine past 3000 rpm – thereby reducing the AFR in the process (Figure 2d) – and advancing the injection timing maintained the rated power of the baseline engine (Figures 2e and 2f). It is worth noting that the dip in torque of

the baseline engine at 4000 rpm is purely due to the fuelling rate (see Figure 2c); the calibration of the twincharged engine rectifies this. The injection timing of the twincharged engine was determined with the objective of minimising brake specific fuel consumption (BSFC). With the fuel injection advanced to this extent, NO_x emissions would be expected to increase; however, due to the limitations of the model and software, any such effect could not be predicted in the simulation. The same applies to any adverse effects the generally low AFR of the twincharged engine may potentially have on exhaust smoke. Nevertheless, in a typical driving cycle during which emissions levels are officially assessed, engine speed and load would not approach the operating points considered in this investigation. Furthermore, in practice an appropriately matched turbocharger – that is, more efficient and designed for purpose – would be expected to alleviate the problems of mass flow capability, and negate the need for injection timing advancement.

The continuously variable supercharger thus shows considerable potential as a pre-boost system to aid downsizing; however, the process of matching further turbo-machinery (such as an efficient, high pressure ratio, narrow mass flow range turbocharger – fixed or variable turbine geometry) to achieve the required increase in rated power (and power density) is beyond the scope of this investigation. Nevertheless, the current results offer the opportunity to use a smaller engine in a given application where low speed driveability is the limiting factor rather than maximum power.

2.3.1 Fuel Consumption

The twincharged system performance improvement came at the cost of deterioration in BSFC while the supercharger was engaged, which is an obvious consequence of the parasitic losses associated with supercharging. As Figure 3 shows, full load BSFC has increased by 4-9% throughout this range. However, since the loads are much higher than those of the baseline engine, it is anticipated that there would be benefits at part load when compared with a conventional engine (of greater displacement) capable of producing similar low speed torque.

2.3.2 Gas Temperatures

Intake air temperatures are shown in Figure 4. The supercharger does have an appreciable effect while it is engaged on the twincharged engine (below 3000 rpm), even with the second intercooler. Above 3000 rpm, when purely turbocharged, intake temperatures return to baseline levels, as would be expected. Exhaust temperatures in the twincharged engine are comparable to the baseline, as shown in Figure 5. The peak temperature of 884 °C at 2500 rpm is well within the temperature limits of current turbine and housing materials [8].

2.3.3 Exhaust Gas Recirculation

The baseline engine has a high pressure (HP) external exhaust gas recirculation (EGR) system, driven by the pressure gradient from exhaust manifold (pre-turbine) to intake manifold (post-compressor). For the sake of simplicity, the EGR rate was set to zero throughout the modelling process, as would be expected on the LTC. As Figure 6 shows, although beneficial in terms of volumetric efficiency, the increase in intake manifold pressure caused by the supercharger would prevent this type of EGR from being used below 2500 rpm. However, depending upon the EGR and supercharger engagement schedules, the original HP EGR system may still be useable at part load. Furthermore, replacing the fixed geometry turbocharger used in the twincharged system with a VGT and closing the turbine vanes would increase the exhaust back pressure and thus improve the pressure gradient from exhaust to intake manifold. Alternatively, if this pressure gradient is still problematic, a low pressure (LP) EGR system (post-turbine to pre-compressor) could be adopted, which would circumvent the issue. LP EGR is currently the focus of considerable research efforts as it offers a number of benefits over conventional HP systems (albeit with its own disadvantages) [17, 18].

2.3.4 CVT Ratio Range

The range of combined gear ratios of the CVT and drive pulley that were applied in the engine model is shown in Figure 7. A ratio range of 2.64:1 was required for the twincharged system, which is well within the capacity of most CVT systems; including traction drives [19]

such as the Milner CVT (MCVT) [20, 21], the Torotrak full toroidal variator [22], the half toroidal variator [23], and the belt drive CVT [24]. However, this ratio range is only taking into account full load conditions; at part load air mass delivery requirements would be proportionally less than these, implying a further required reduction in supercharger drive ratio. The necessary extension to the ratio range would depend on the control strategy employed for engaging the supercharger. In an earlier study by Schmitz et al. [6] a positive displacement-type supercharger was driven via an electromagnetic clutch and bypass arrangement to boost the performance of a turbocharged heavy duty diesel engine. In this instance the supercharger was engaged during all transient and steady state conditions below a set speed threshold, and was also engaged in transient conditions above the threshold when boost pressure was less than the demanded value, Table 4 shows the rules used to implement this scheme.

The overall ratio required to drive the supercharger is significant. Table 5 summarises how these ratios might be achieved for typical existing CVT systems, using a speed up pulley drive, and an intermediate step up between the CVT and the turbo-machinery. Experience suggests that most traction drive CVTs are capable of being driven at up to 10000 rpm, indicating a drive pulley ratio up to 3.5 as being appropriate, depending on engine disengagement speed; while the belt drive CVT is typically limited to 6000 rpm, due to centripetal belt forces. The requirement for the step up ratio between the CVT output and supercharger input will then be a function of the CVT ratio. This ratio will be dependent on the turbo-machinery design speed and the ratio of the CVT. For example most traction drives and the belt drive ratio spread is symmetrical through unity (1:1) ratio, the MCVT range is biased to typically below 1.6~2:1. From Table 5 it can be seen that the ratio requirement for the step up system is significantly less for the MCVT compared to the full and half toroidal drives, and significantly higher again for the belt drive. This may have considerable implications for transient performance, where the acceleration torque (due to supercharger inertia) will be factored by the square of the step up. However, the full and half toroid designs

and the belt drive typically have a higher ratio range, although work has been undertaken to derive MCVT concepts with greater ratio range [25, 26]. Increased ratio range is likely to be beneficial in lower load operating conditions where turbo-machinery speeds will be reduced.

2.3.5 CVT Efficiency

During the initial model development the CVT efficiency was assumed to be 100% to simplify analysis – the object of this project was to investigate the potential of the general concept rather than constrain the concept to a specific type of CVT at this stage. Figure 8 shows the influence of CVT efficiency on the torque curve of the twincharged system, indicating that for typical efficiency values [20] there is little impact on overall performance – a CVT efficiency of 85% resulting in a reduction in peak torque of 2%.

3 Transient Simulation

A further aspect of air handling system performance is its capability to respond during transient events. The aim of this part of the investigation was to predict the response to a fixed speed 'tip-in' transient – i.e. a step in fuel quantity from a low to high value. This is designed to simulate the driver depressing the accelerator pedal – or 'tipping-in' – at light load and demanding full load from the engine [5].

3.1 Simulation Setup

To undertake this work the WAVE engine models were integrated in to a co-simulation environment with Simulink to control the engine actuators in response to sensors defined in the engine model. A block diagram was constructed around the twincharged engine architecture (with original supercharger compressor) with engine speed and fuel demand as the main user input parameters. From the mass air flow (MAF) sensor, an AFR/smoke limit feedback loop was created. Boost demand and CVT ratio maps were developed based on the respective values from the full load steady state results. These were included as lookup tables as part of a boost demand feedback loop in the block diagram – a proportional-integral (PI) controller was used to convert the boost error into a CVT ratio, which was then added to

the value from the CVT ratio lookup table (essentially providing a basic ‘feed-forward’ action). A function was also included to limit the rate of change of CVT ratio, since it cannot realistically change instantaneously. Turbocharger speed, peak cylinder pressure, and turbine inlet temperature were also monitored. Figure 9 shows the complete block diagram for the twincharged engine simulation. A similar model was developed for the baseline engine. The boost demand lookup table was updated with the relevant full load steady state data, and a PI controller was developed to drive the VGT rack position actuator.

Both the baseline and optimised twincharged models were then tested using a step in fuel demand from 10 mg/injection to an upper value which was dependent on engine speed. For the baseline engine, these upper values were determined from the steady state LTC. As for the twincharged engine, the following logic was applied to allow a more direct comparison: where equal or greater torque was produced, the same fuel values as the baseline were used; otherwise, the fuelling was increased to produce the same torque as the baseline (this was only required at the 1750 and 2000 rpm test points). In all cases the fuel demand was set to a constant 10 mg/injection for the first two seconds to allow the simulation to stabilise prior to commencing the tip-in. Tests were performed at 250 rpm intervals from 1000-2000 rpm inclusive.

3.1.1 CVT Ratio Control

The linearly interpolated lookup tables that were constructed for boost demand and CVT ratio ‘feed-forward’ action were perhaps a little simplistic, as was the tuning of the PI controllers – although their performance was deemed satisfactory for the purpose of this investigation. Improved transient response may be achieved if more effort were spent on this task; however, it is likely that this would best be done with physical hardware.

A more crucial feature was the simplified rate of change of CVT ratio. This was modelled by a simple linear rate limit block, with an allowable rate-of-change of +/- 320 per second. This value was reached from the assumption that the ratio change of 200:1-40:1 could be

achieved in 0.5 seconds, and hence this ratio gap could be traversed twice in one second. From experience of the MCVT this is a realistic target and adequately demonstrates the concept.

3.2 Simulation Results

At the lower engine speeds the difference in boost response between the baseline and twincharged engines was clearly evident; at 1250 rpm the twincharged engine achieving the boost demand in less than 0.5 seconds compared with around 1.25 seconds for the baseline engine (Figure 10a), despite the demanded boost being significantly higher. As engine speed increased, the performance deficit between the models gradually decreased, with the response time reduced to 0.6 seconds at 2000 rpm for the baseline engine (Figure 10c).

The difference in transient response between the two systems is also demonstrated in the turbo-machinery speeds, shown in Figure 11. Despite the VGT system, the turbocharger of the baseline engine accelerates at a much lower rate than the supercharger of the twincharged engine, Figure 11a. Considering the torque response of the two systems at 1250 rpm (Figure 12a), not only does the twincharged engine reach its peak torque in less than half the time of the baseline engine, but its final magnitude is also greater. This would present clear benefits in driveability of the vehicle through enhanced acceleration response. As engine speed is increased, the twincharged system retains its superiority in terms of transient torque response, although this is significantly reduced as engine speed reaches 2000 rpm (Figure 12c). Since the VGT mechanism was disabled in the twincharged model in order to simulate the behaviour of a fixed geometry turbocharger, the speed (and thus boost pressure) of the turbocharger in the twincharged system is negligible at these engine speeds (Figure 11). It is expected that greater performance could be extracted from the twincharged scheme if the VGT system was incorporated and appropriately calibrated.

The phenomenon in torque response around 0.2 seconds into the transient as shown in Figure 12 is due to the slight delay in boost response to the instantaneous step in fuel

demand – this can be seen to a lesser extent in Figure 10, where there is a slight lag in boost response in each test case. For the twincharged engine, the fluctuating supercharger power requirement is also a major factor in this uneven behaviour, as shown in Figure 13. Figure 13a is the engine brake torque response for each of the engine speeds tested, displayed at a higher resolution in time than Figure 12; Figure 13b is the torque (at the crankshaft) required to accelerate the supercharger, proportional to the inertia of the supercharger system rotating mass; Figure 13c is the crankshaft torque required to overcome the aerodynamic load on the supercharger compressor, which relates to supercharger speed. Supercharger inertia was assumed to be the same as the original turbocharger, but scaled according the aforementioned relationship in Equation (5) using the supercharger scaling factor (given in Table 3). The total turbocharger inertia was used in order to account for the inertia of the drive system – i.e. shafts, belts and pulleys – as well as the compressor itself. The inertia of the CVT was ignored, as this would depend both on the particular CVT system used, and on the varying transmission ratio. Consequently, the magnitude of the inertia torque would in reality be higher than in Figure 13b. Nevertheless, even factoring in an increase in system inertia, the input torque demand on the CVT (with an input drive ratio such as those listed in Table 5) would be within the capacity of most systems, and it is anticipated that the torque response of the engine would not be significantly diminished. Regarding the aforementioned uneven torque behaviour at the beginning of the transient, appropriate calibration of the control and fuelling systems would be expected to rectify this.

For all of the test speeds the CVT ratio ranges were within the operational limits proposed earlier (Figure 14). Figure 15 shows the transient AFR during the tip in processes at 1000 rpm and 2000 rpm. The twincharged engine tended to operate at higher AFRs and avoided running into the limit, which is likely to be beneficial in terms of improved transient smoke emissions, as well as showing potential for increasing the fuelling to bring the performance in line with the steady state LTC. The spike in the twincharged AFR around 0.25 seconds into

the transient in Figure 15a is due to slight overshoot of the supercharger – compare with Figure 11a.

4 Conclusions

4.1 Steady State Performance

The potential for the augmentation of the low speed torque of a VGT-equipped high speed diesel engine has been demonstrated by employing a compound charging system (twincharged) using a combination of CVT driven supercharger and fixed geometry turbocharger. The original turbo-machinery was used as the foundation for the twincharged scheme, and scaled in simulation. Design of experiments and optimisation techniques were used to find optimal settings for the size of the turbo-machinery. It was found that the addition of a supercharger bypass arrangement avoided the flow range limitations (and parasitic losses) of the supercharger at high engine speeds (above 3000 rpm). This arrangement enabled the turbocharger performance to be fully exploited at higher engine speeds. Peak torque was improved by 15%, with 90% of the peak value available at 1000 rpm, compared with 50% for the baseline engine. Rated power, however, was not increased – a result of effectively using the original VGT as an inefficient fixed geometry unit away from the turbine design conditions. Using an appropriately matched turbocharger would be expected to rectify this. Brake specific fuel consumption increased by up to 9% while the supercharger was engaged, a result of the parasitic losses associated with mechanical supercharging. However, baseline levels were restored beyond the supercharger disengagement speed. Gas temperatures throughout the twincharged engine were comparable to baseline levels.

The supercharger drive ratio range required for the twincharged engine was investigated and found to be well within the capability of a range of CVT systems; a number of drive combinations were proposed to achieve the required overall drive ratio. CVT mechanical efficiencies were ignored throughout the investigation, but for typical values they were shown to have little overall impact on performance.

4.2 Transient Performance

Transient performance of the proposed twincharged system was compared to the baseline engine in a Simulink co-simulation environment with the engine models. The twincharged system displayed significant improvement in transient response with improved boost response and an associated improvement in transient torque response, which would result in significantly improved vehicle acceleration and driveability. Transient AFR was also improved, which is likely to be demonstrated by reduced visible smoke during tip-in manoeuvres, as well as showing potential for increasing the fuelling to bring the transient torque in line with the improved steady state LTC.

4.3 Further Work

Since the potential performance benefits of the twincharged system were established using scaled versions of the original turbo-machinery, commercially available units should be investigated to explore whether further gains are achievable. In particular, using a more efficient turbocharger capable of high pressure ratios (and preferably VGT) should be explored to achieve the increased rated power (and high power density) required for downsizing. The project scope could also be broadened to develop a part load control strategy, with the by-product of establishing and validating the required CVT ratio range.

Acknowledgements

The authors would like to acknowledge the Engineering and Physical Sciences Research Council (EPSRC) for funding this research under projects EP/C540883/1 and EP/C540891/1 and also the Ford Motor Company for assisting with the research in terms of initial model development and advice throughout the project.

References

[1] **European Commission.** *Setting emission performance standards for new passenger cars as part of the Community's integrated approach to reduce CO2 emissions from light-duty vehicles*. Regulation (EC) No 443/2009, 2009.

[2] **United States Environmental Protection Agency.** *EPA and NHTSA Finalize Historic National Program to Reduce Greenhouse Gases and Improve Fuel Economy for Cars and Trucks*. Regulatory Announcement EPA-420-F-10-014, 2010.

[3] **European Communities.** *Commission proposal to limit the CO2 emissions from cars to help fight climate change, reduce fuel costs and increase European competitiveness.* EUROPA press release IP/07/1965, 2007.

[4] **Hancock, R., Fraser, N., Jeremy, M., Sykes, R.** and **Blaxill, H.** A New 3 Cylinder 1.2l Advanced Downsizing Technology Demonstrator Engine. SAE paper 2008-01-0611, 2008.

[5] **Wijetunge, R., Criddle, M., Dixon, J.** and **Morris, G.** Comparative Performance of Boosting Systems for a High Output, Small Capacity Diesel Engine. STA paper F2004F195, 2004.

[6] **Schmitz, T., Holloh, K., Juergens, R.** and **Fleckenstein, G.** Potential of Additional Supercharging for Commercial Vehicle Engines. SAE paper 942268, 1994.

[7] **Matsura, Y., Nakazawa, N., Kobayashi, Y., Ogita, H.** and **Kawatani, T.** Effects of Various Methods for Improving Vehicle Startability and Transient Response of Turbocharged Diesel Trucks. SAE paper 920044, 1992.

[8] **Baines, N.C.** *Fundamentals of Turbocharging*, 2005 (Concepts NREC, Vermont).

[9] **Bhinder, F.S.** Supercharging Compressors – Problems and Potential of the Various Alternatives. SAE paper 840243, 1984.

[10] **Tomita, T., Ikeya, N., Ishihara, D., Kondoh, N.** and **Ohkita, A.** Hybrid Charging System for Heavy Duty Diesel Engines. SAE paper 910419, 1991.

[11] **Whitworth, B.** Doppelgänger. *Automotive Engineer*, May 2006, pp. 37-38 (Professional Engineering Publishing Ltd, London).

[12] **Akehurst, S.** and **Piddock, M.** A Multiple Factor Simulation and Emulation Approach to Investigate Advanced Air Handling Systems for Future Diesel Engines. SAE paper 2008-01-0297, 2008.

[13] **Ricardo Software.** *Ricardo WAVE 7.2 – Engine Manual*, 2006.

[14] **Watson, N.** and **Janota, M.S.** *Turbocharging the Internal Combustion Engine*, 1982 (Macmillan Publishers Ltd, Basingstoke).

[15] **Thirouard, M., Mendez, S., Pacaud, P., Chmielarczyk, V., Ambrazas, D, Garsi, C., Lavoisier, F.** and **Barbeau, B.** Potential to Improve Specific Power Using Very High Injection Pressure in HSDI Diesel Engines. SAE paper 2009-01-1524, 2009.

[16] **Millo, F., Mallamo, F., Pautasso, E.** and **Ganio Mego, G.** The Potential of Electric Exhaust Gas Turbocharging for HD Diesel Engines. SAE paper 2006-01-0437, 2006.

[17] **Maiboom, A., Tauzia, X., Rahman Shah, S.** and **Hétet, J.** Experimental Study of an LP EGR System on an Automotive Diesel Engine, compared to HP EGR with respect to PM and NOx Emissions and Specific Fuel Consumption. In Proceedings of 9th International Conference on Engines and Vehicles, Naples, Italy, 14-17 September 2009, paper 2009-24-0138 (Consiglio Nazionale delle Richerche, Naples).

[18] **Beatrice, C., Bertoli, C., Del Giacomo, N.** and **Guido, C.** Experimental Investigation of the Benefits of Cooled and Extra-cooled Low-Pressure EGR on a Light Duty Diesel Engine Performance. In Proceedings of 9th International Conference on Engines and Vehicles, Naples, Italy, 14-17 September 2009, paper 2009-24-0126 (Consiglio Nazionale delle Richerche, Naples).

[19] **Akehurst, S., Parker, D. A.** and **Schaaf, S.** CVT Rolling Traction Drives – A Review of Research Into Their Design, Functionality, and Modelling. *Transactions of the ASME, Journal of Mechanical Design*, 2006, **128**(5), 1165-1176.

[20] **Akehurst, S., Brace, C.J., Vaughan, N.D., Milner, P.** and **Hosoi, Y.** Performance Investigations of a Novel Rolling Traction CVT. SAE paper 2001-01-0874, 2001.

[21] **Akehurst, S., Parker, D.A.** and **Schaaf, S.** Dynamic Modelling of the Milner Continuously Variable Transmission – The Basic Kinematics. *Transactions of the ASME, Journal of Mechanical Design*, 2007, **129**(11), 1170-1178.

[22] **Lee, A.P., Newall, J., Ono, Y.** and **Hoshino, T.** Developing the Durability of a Dual-Cavity Full-Toroidal IVT Variator. SAE paper 2002-01-0587, 2002.

[23] **Tanaka, H., Toyoda, N., Machida, H.** and **Imanishi, T.** Development of a 6 Power-Roller Half-Toroidal CVT – Mechanism and Efficiency. In International Continuously Variable and Hybrid Transmission Congress, California, 23-25 September 2004, paper 04CVT-36.

[24] **Akehurst, S.** Investigating the loss mechanisms associated with a pushing metal V-belt CVT. PhD thesis, University of Bath, Bath, 2001.

[25] **Akehurst, S.**, **Moyers, J.**, **Hunt, A.** and **Schaaf, S**. Development of a design tool for modelling and optimisation of the Milner CVT. In JSME International Conference on Motion and Power Transmission, Japan, 13-15 May 2009.

[26] **Akehurst, S.** Optimizing the Design of a Milner CVT Using Simulation Based Design of Experiments. In SAE 2009 World Congress, Detroit, Michigan, 20-23 April 2009.

Tables

Table 1 Baseline engine parameters

Parameter	*Value*
Bore (mm)	86
Stroke (mm)	86
Con Rod Length (mm)	152
Compression Ratio	19:1
Max Power (kW) @ Rated Speed (rpm)	96, 4000
Max Torque (Nm) @ Rated Speed (rpm)	330, 1900

Table 2 Design of Experiments factors

Parameter	*Min*	*Max*
SC factor	0.8	1.1
TC factor	0.9	1.2
TT factor	0.9	1.2
CR	16	19
CVT ratio	0	250
Engine speed	1000 rpm	4500 rpm
AFR	17	22
SOI	-30	0

Table 3 Optimised design parameters

Parameter	*Optimised Value*
SC factor	0.90
TC factor	1.075
TT factor	0.93
CR	18

Table 4 Decision map for supercharger engagement (data reproduced from Schmitz et al. [6])

Operating Condition	*Criteria*	*Magnetic Clutch*
Engine start	Engine speed = 0; ignition on	Disengaged
Vehicle stand still	Vehicle speed = 0; engine idling; gearbox in neutral	Disengaged
Vehicle start	Vehicle speed = 0; engine idling; gear engaged	Engaged
Engine speed < 1100 rpm steady state and transient	Engine speed	Engaged
Engine speed > 1100 rpm steady state	Boost pressure = rated value of accelerator position	Disengaged
Engine speed > 1100 rpm transient	Boost pressure ≤ rated value of accelerator position	Engaged
Engine braking operation	Switch on	Engaged

Table 5 CVT ratio ranges to match turbo-machinery

Parameter	*Milner CVT*	*Full Toroidal CVT Half Toroidal CVT*	*Belt Drive CVT*
Input speed limit (rpm)	10000	10000	6000
Input drive ratio	3.5	3.5	2
CVT ratio range	4.5	6	6
Min CVT ratio	2	0.41	0.4
Max CVT ratio	9	2.45	2.5
Step up ratio	5.6	20.5	35
Min overall ratio	39.2	29.3	28
Max overall ratio	176.4	175.8	175

Figures

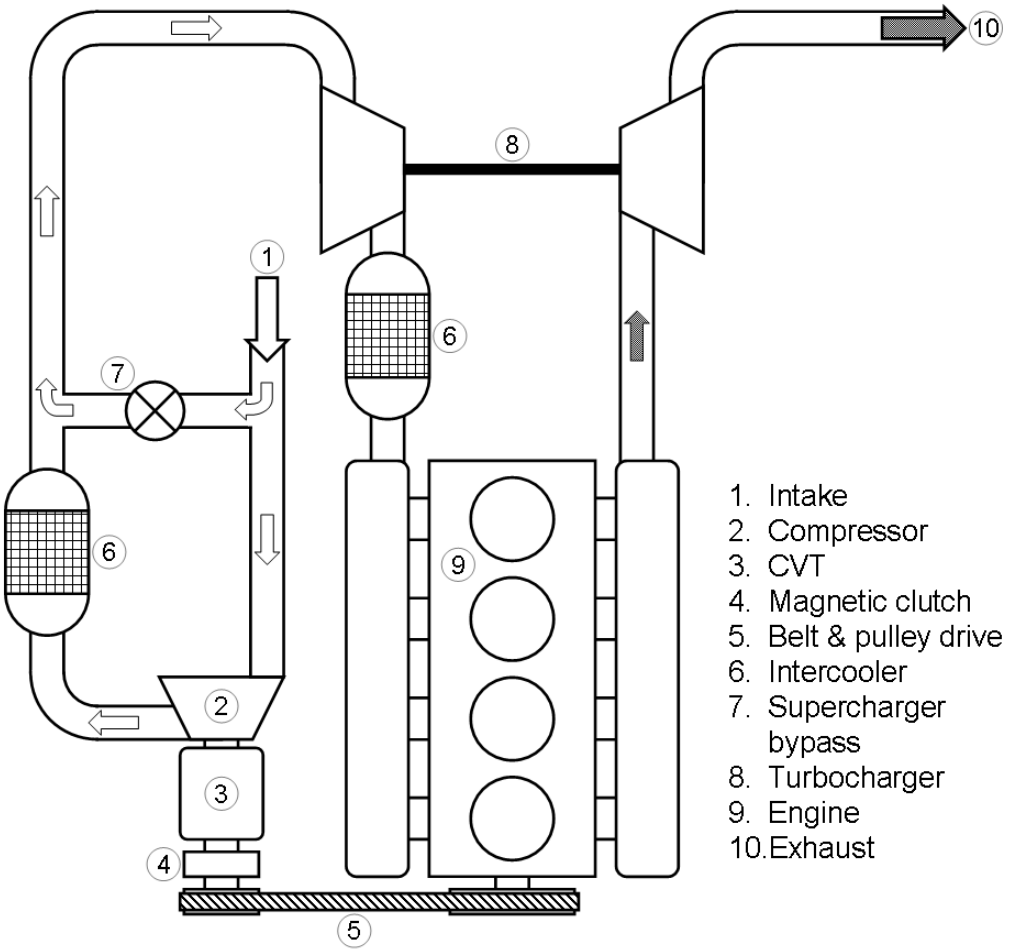

Figure 1 Schematic diagram of the proposed twincharged engine

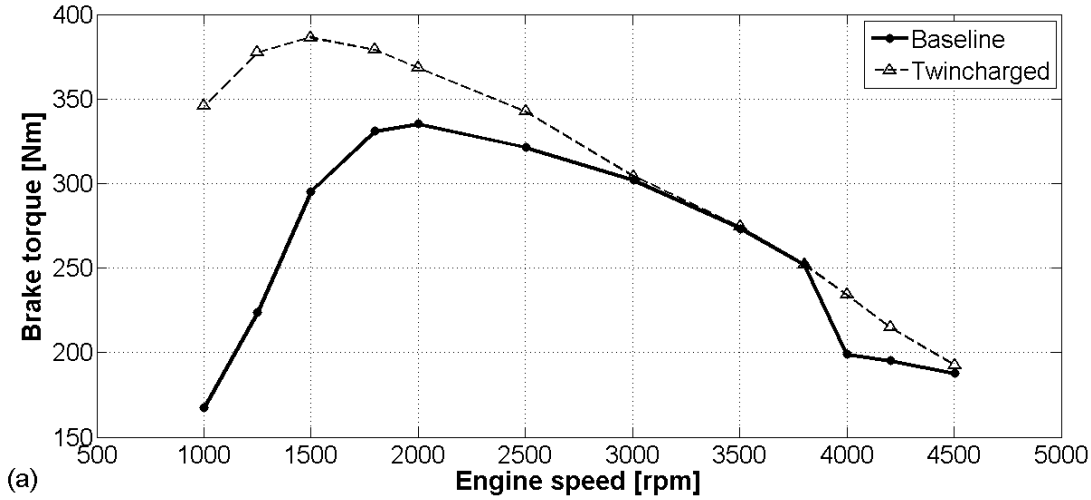

(a)

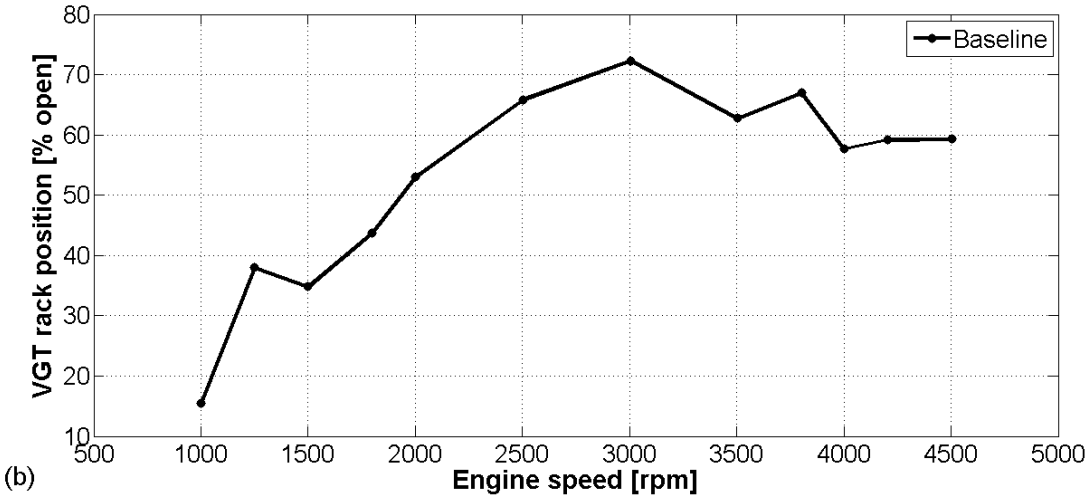
Baseline
VGT rack position [% open]
Engine speed [rpm]

(b)

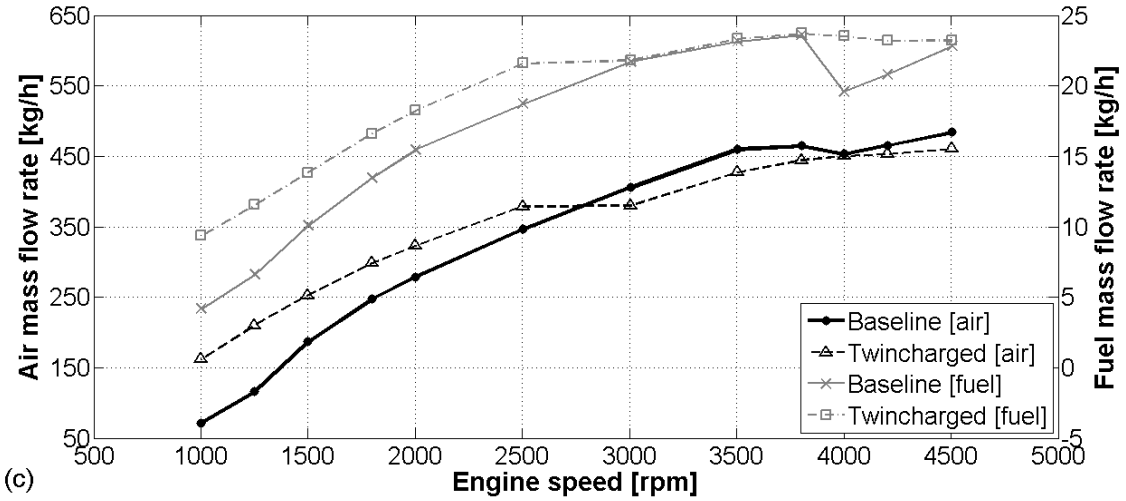
Baseline [air]
Twincharged [air]
Baseline [fuel]
Twincharged [fuel]
Air mass flow rate [kg/h]
Fuel mass flow rate [kg/h]
Engine speed [rpm]

(c)

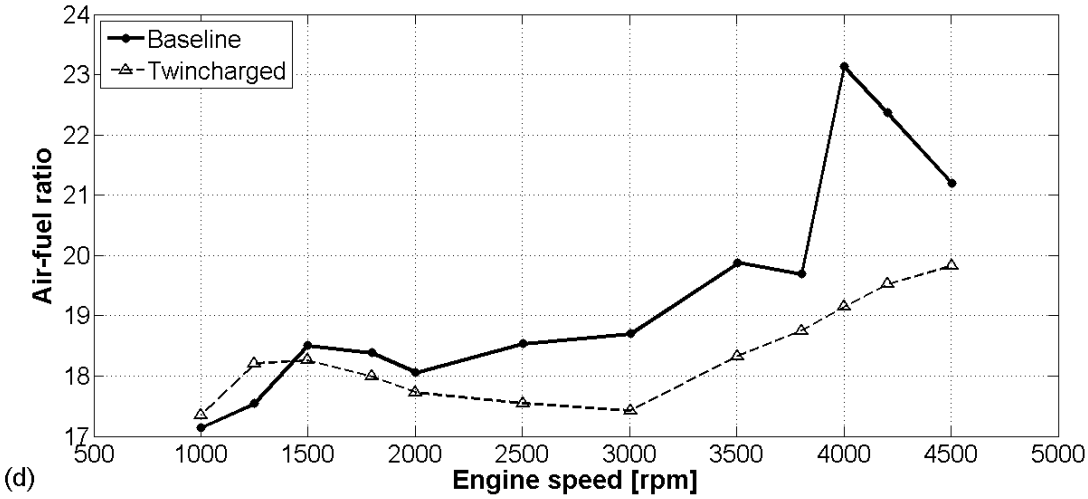
Baseline
Twincharged
Air-fuel ratio
Engine speed [rpm]

(d)

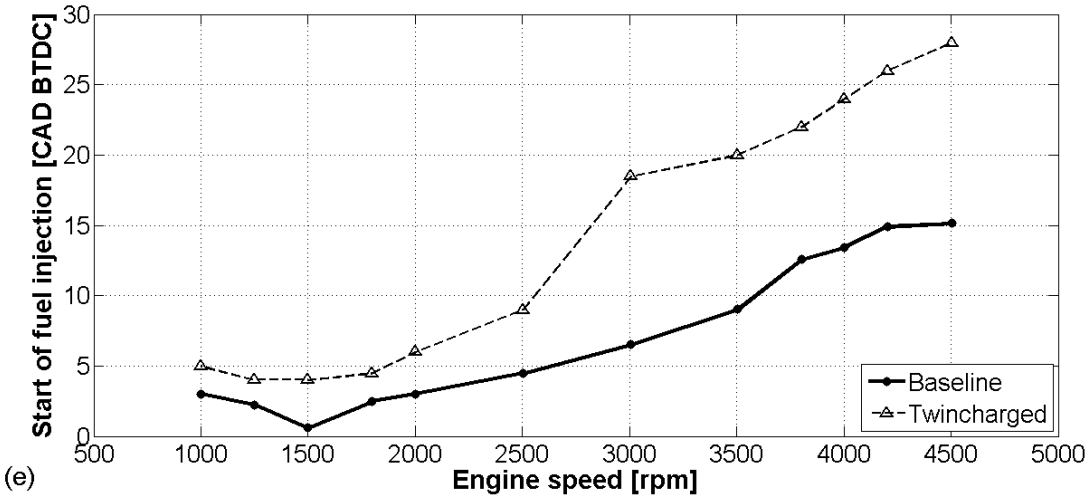

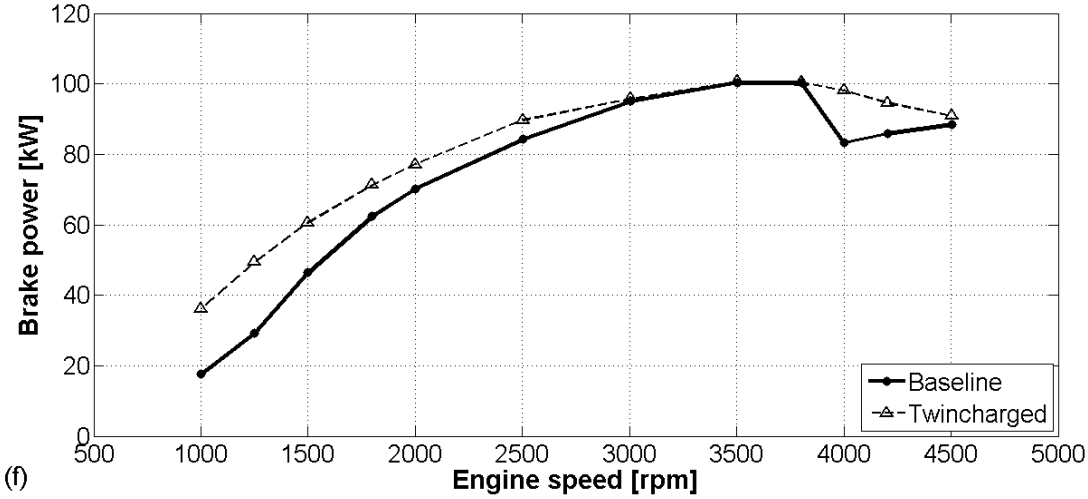

Figure 2 Steady state results – a) torque; b) baseline VGT rack position; c) air and fuel mass flow; d) AFR; e) fuel injection timing; f) power

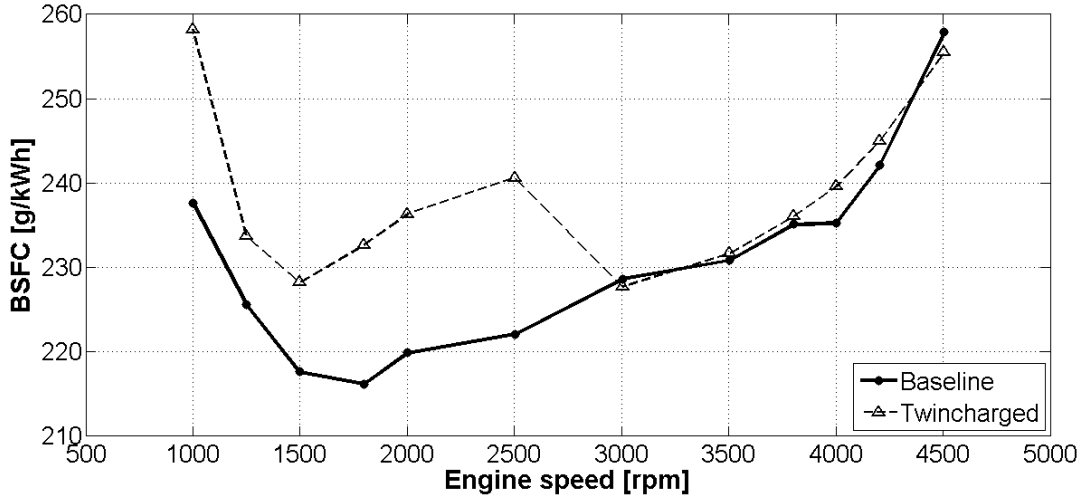

Figure 3 Steady state results – BSFC

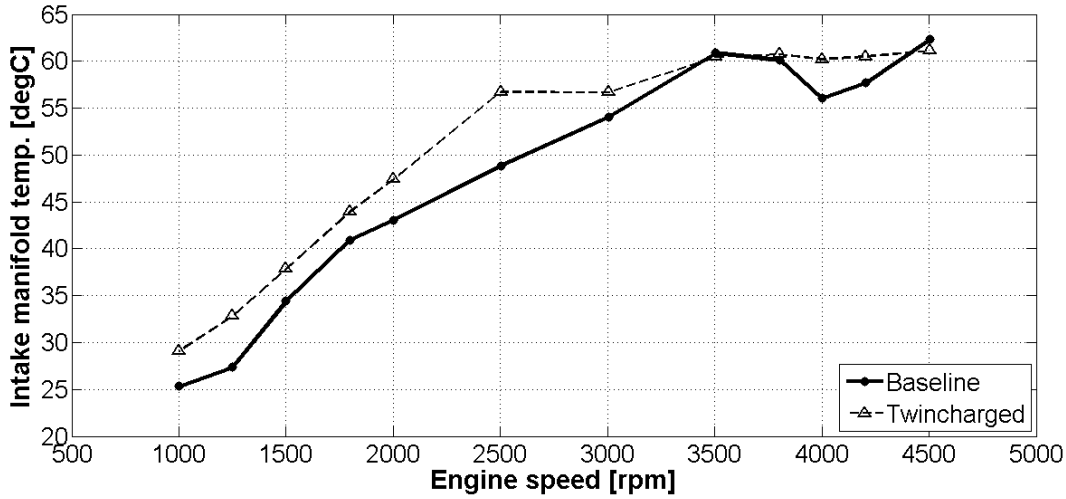

Figure 4 Steady state results – intake manifold temperature

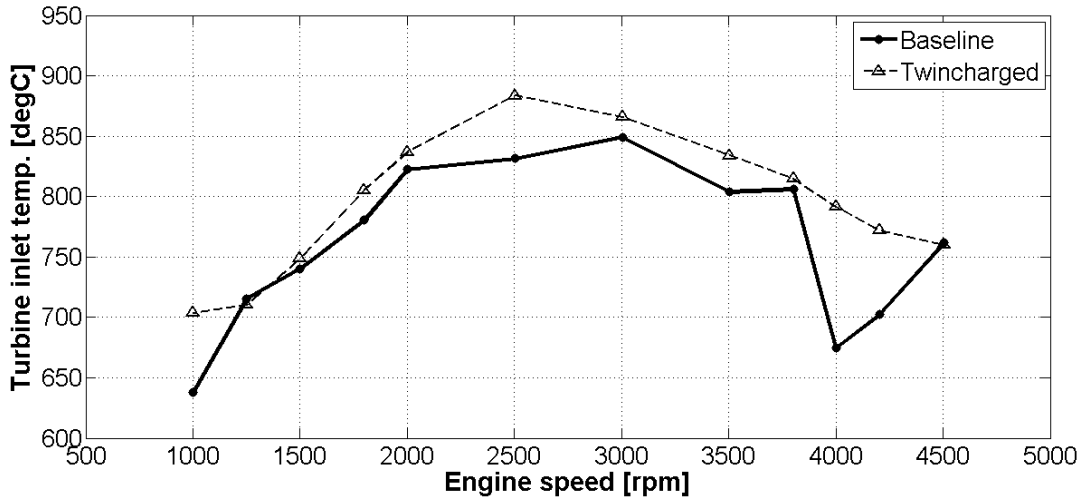

Figure 5 Steady state results – turbine inlet temperature

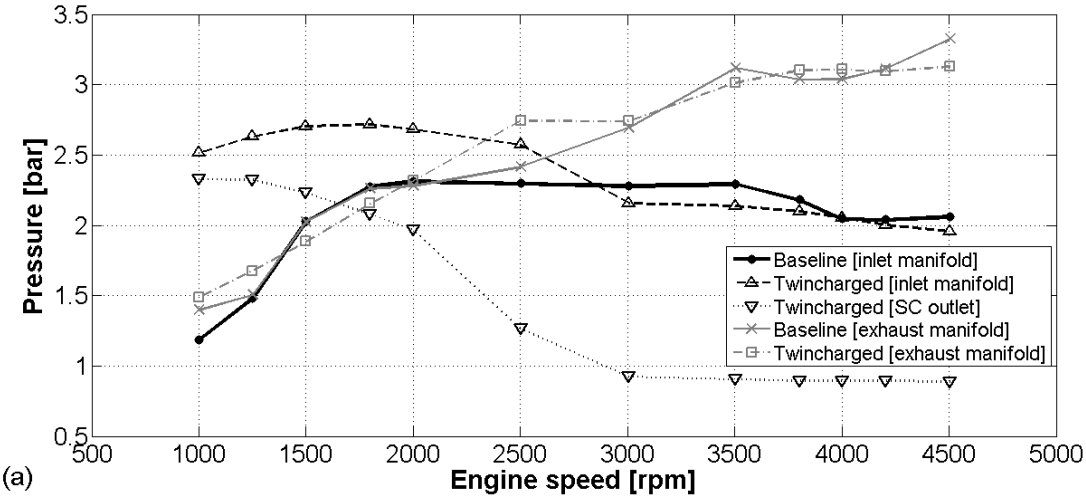

(a)

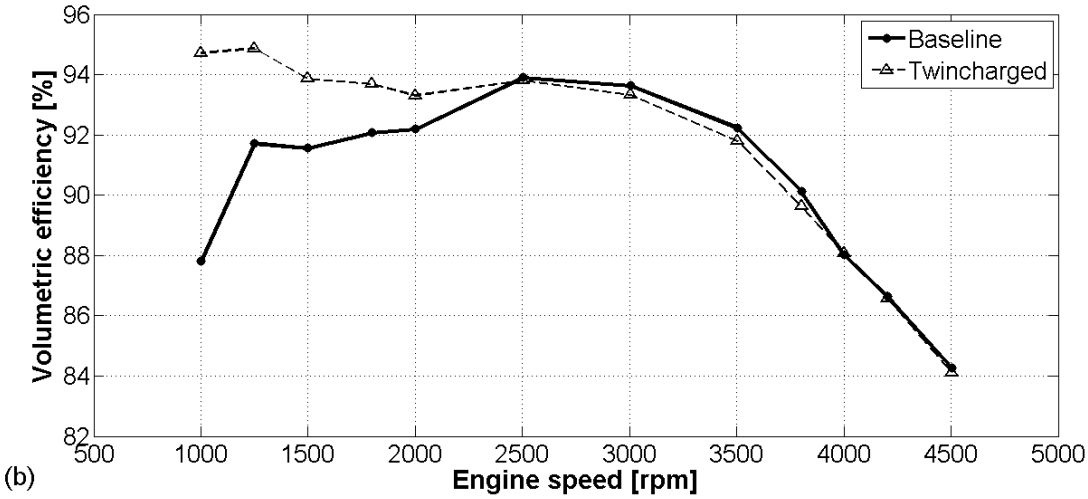

Figure 6 Steady state results – a) inlet and exhaust manifold pressures; b) volumetric efficiency (relative to inlet manifold conditions)

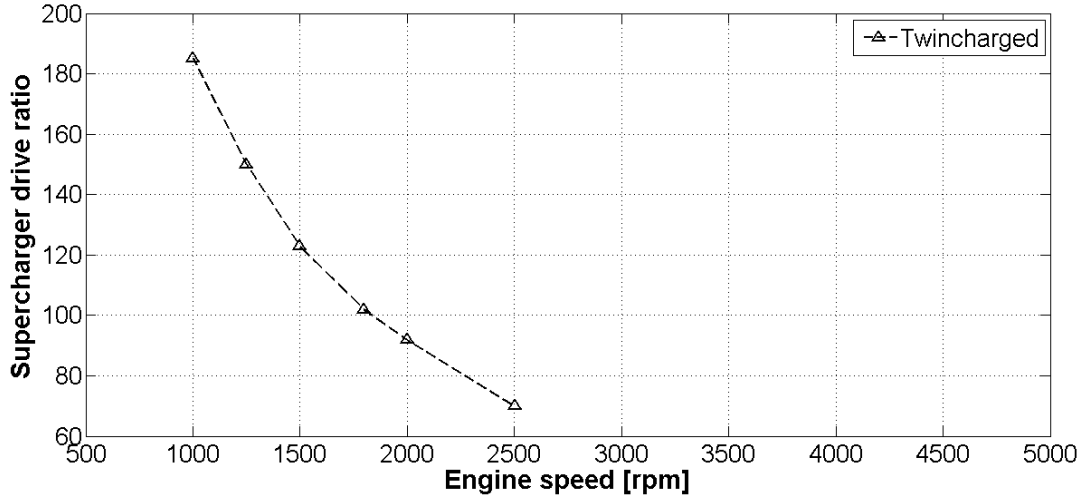

Figure 7 CVT ratio range

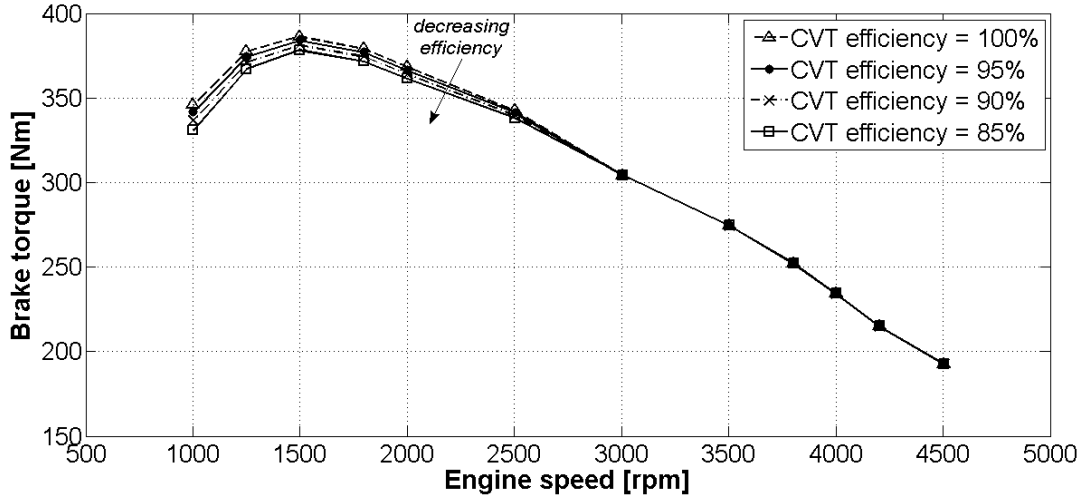

Figure 8 Effect of CVT efficiency

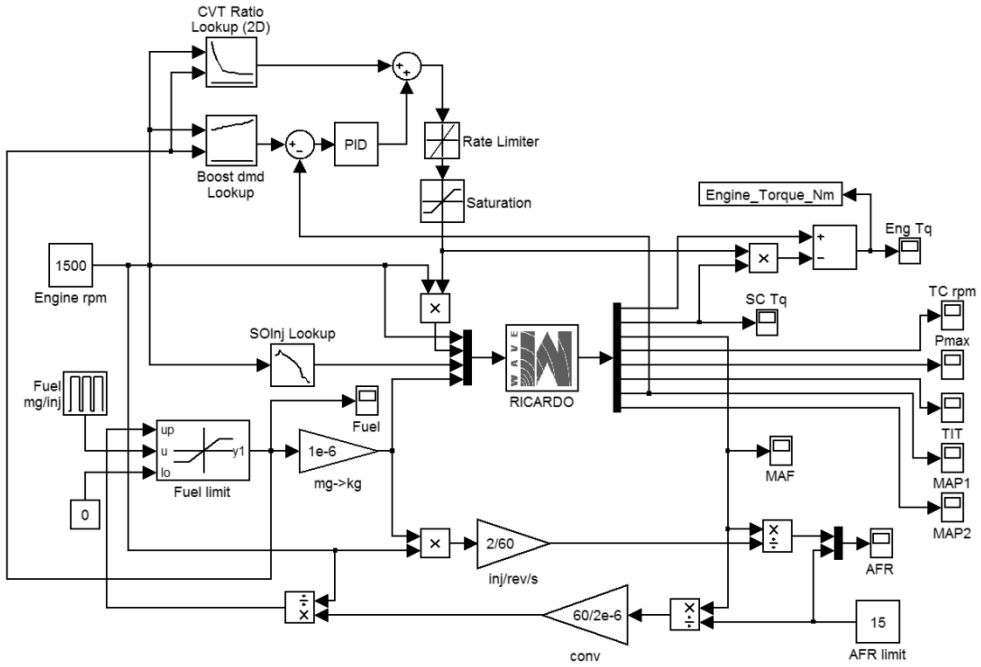

Figure 9 Simulink block diagram – twincharged engine

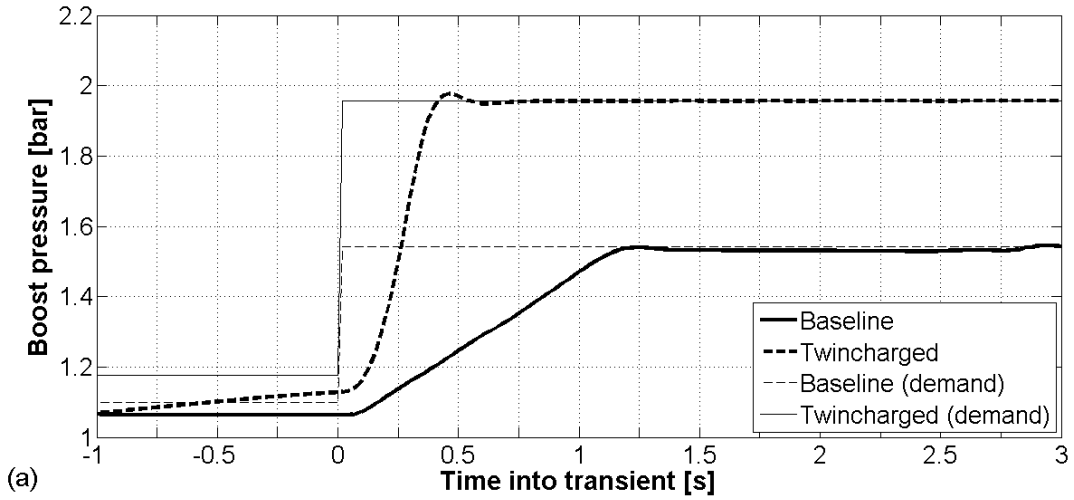

(a)

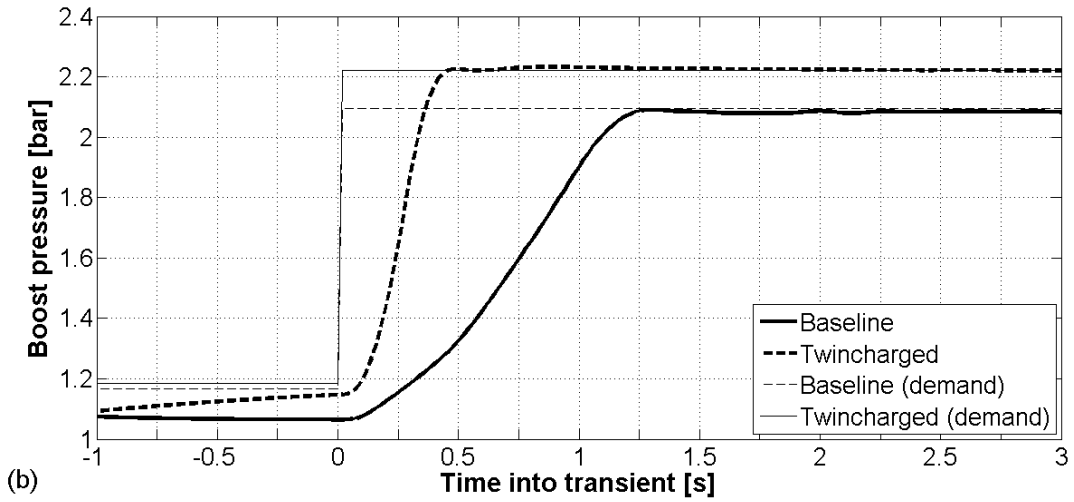

(b)

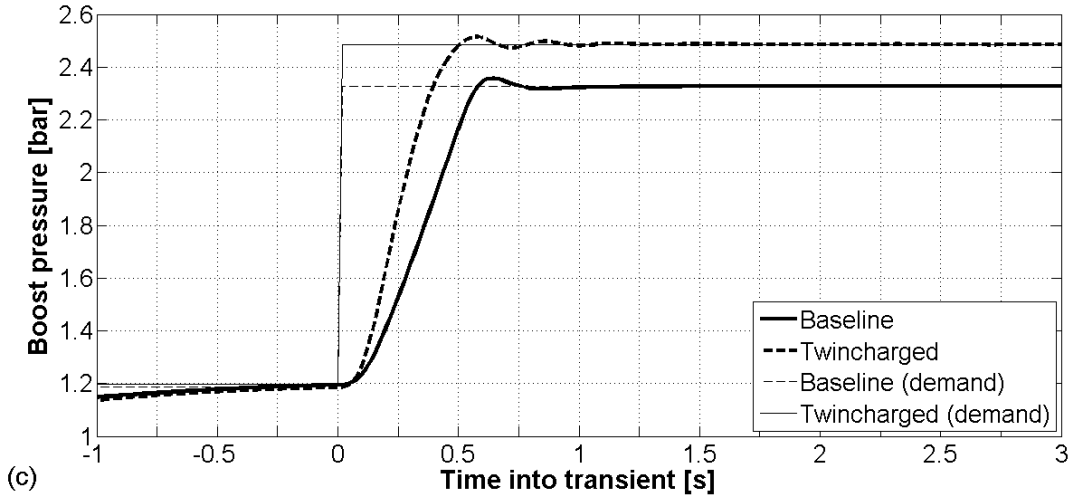

Figure 10 Transient boost response – a) 1250 rpm; b) 1500 rpm; c) 2000 rpm

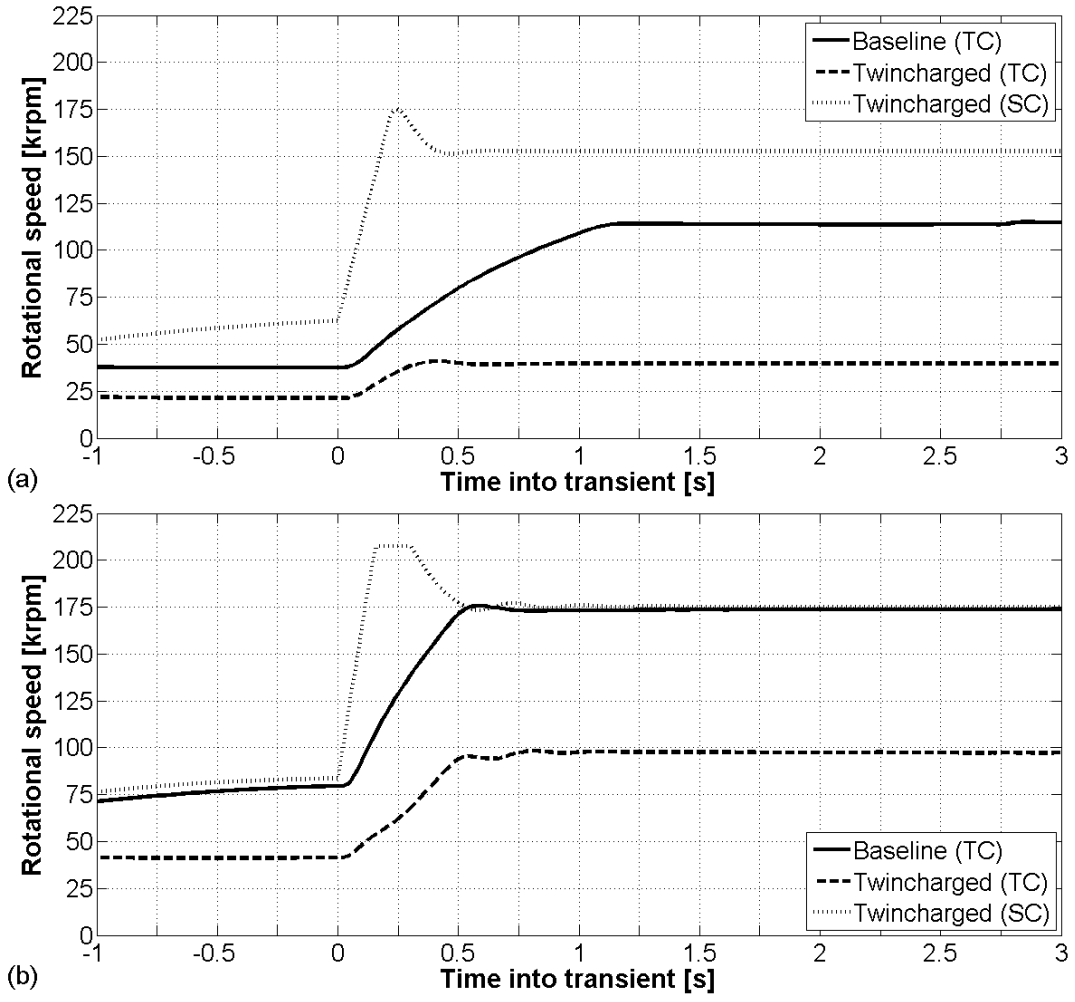

Figure 11 Transient turbocharger and supercharger speeds – a) 1250 rpm; b) 2000 rpm

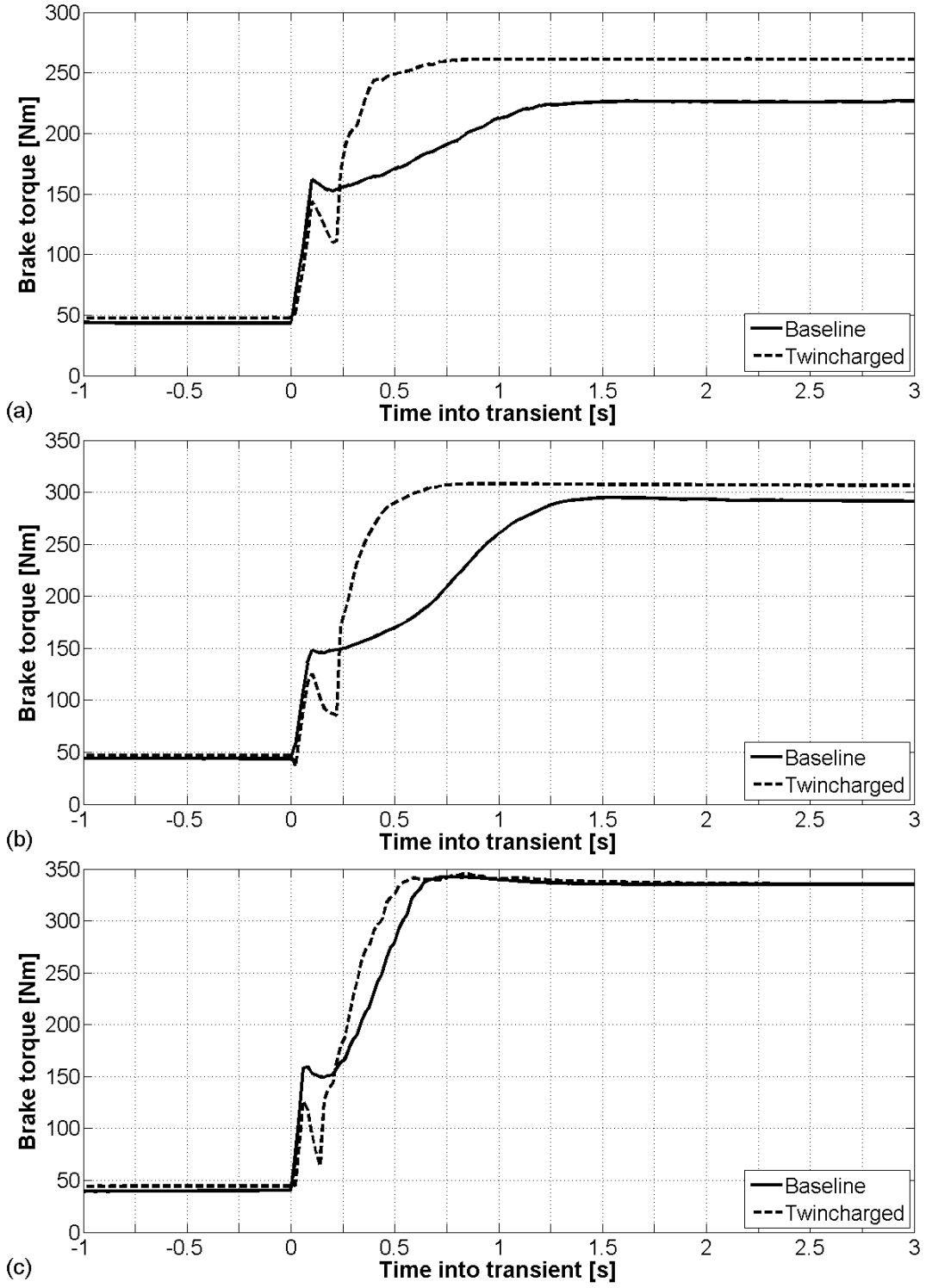

Figure 12 Transient torque response – a) 1250 rpm; b) 1500 rpm; c) 2000 rpm

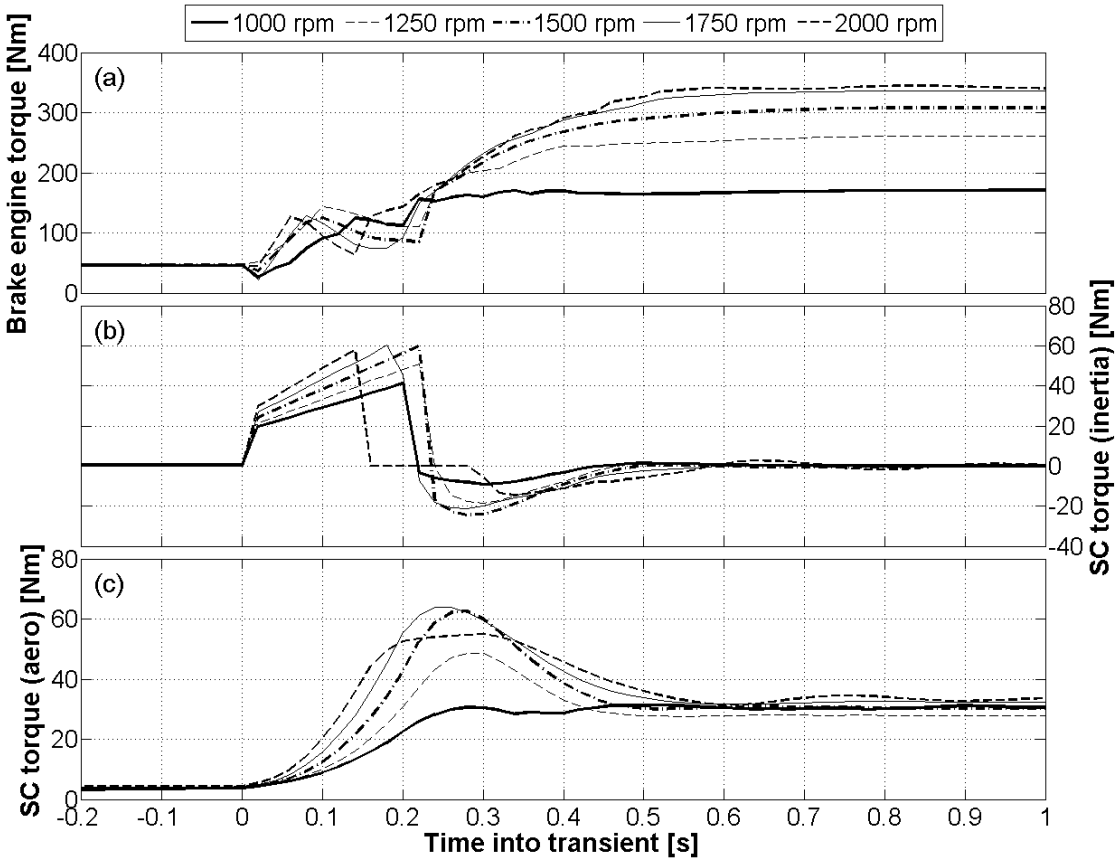

Figure 13 Twincharged engine transient torque – a) brake engine torque; b) supercharger inertia torque demand; c) supercharger aerodynamic torque demand

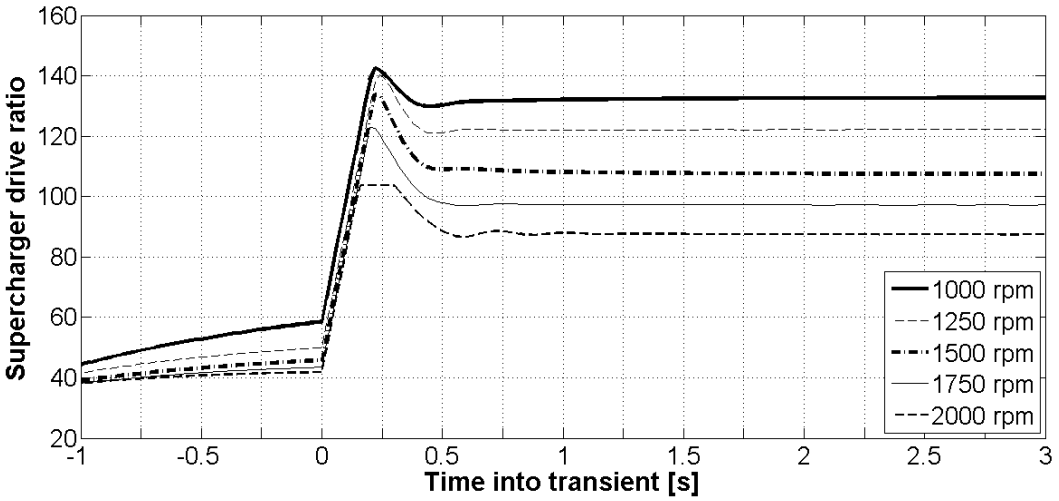

Figure 14 Twincharged engine CVT ratio range

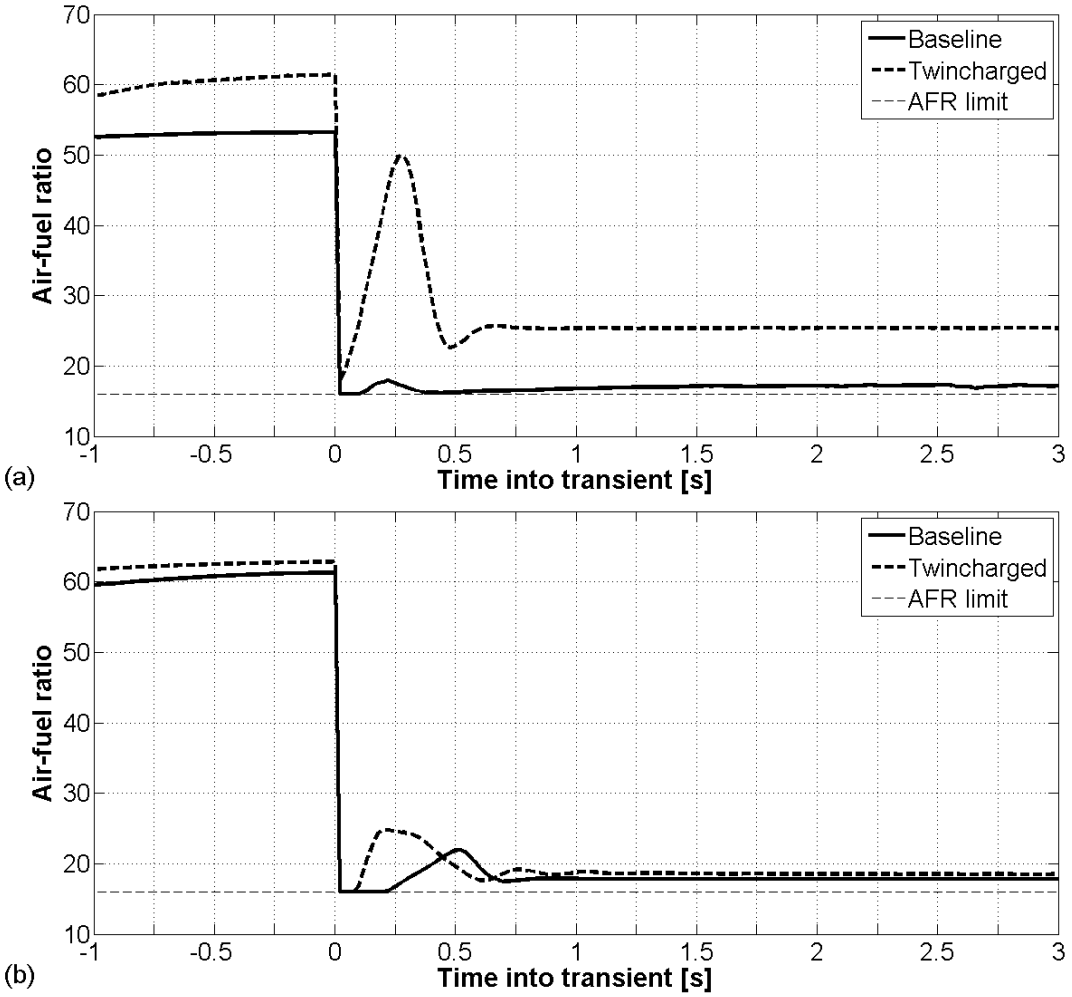

Figure 15 Transient AFR – a) 1000 rpm; b) 2000 rpm

Appendix

Acronyms

AFR	air-fuel ratio
BSFC	brake specific fuel consumption
CAGE	Calibration Generation
CR	compression ratio
CVT	continuously variable transmission
DoE	design of experiments
EGR	exhaust gas recirculation
HP	high pressure
HSDI	high speed direct injection
LP	low pressure
LTC	limiting torque curve
MAF	mass air flow (sensor)
MBC	Model-Based Calibration Toolbox
MCVT	Milner continuously variable transmission
NO_x	oxides of nitrogen
PI	proportional-integral (control)
SC	supercharger compressor
SF	scaling factor
SOI	start of injection (fuel)
TC	turbocharger compressor
TT	turbocharger turbine
VGT	variable geometry turbocharger

Notation

d	diameter (m)
$\dot{m}$	mass air flow (kg/s)
n	speed (rad/s)
I	inertia (kgm^2)
P	pressure (N/m^2)
T	temperature (K)
τ	torque (Nm)

Subscripts

act	actual

comp	compressor
corr	corrected
in	inlet
ref	reference
turb	turbine